

Magnetism and structure of $\text{Zn}_x\text{Fe}_{3-x}\text{O}_4$ films processed via spin-spray deposition

Mitra Taheri

Department of Materials Science and Engineering, Carnegie Mellon University, Pittsburgh, Pennsylvania 15231

E. E. Carpenter, V. Cestone, M. M. Miller, and M. P. Raphael

Materials Physics Branch, Naval Research Laboratory, Washington, DC 20375

M. E. McHenry

Department of Materials Science and Engineering, Carnegie Mellon University, Pittsburgh, Pennsylvania 15231

V. G. Harris^{a)}

Materials Physics Branch, Naval Research Laboratory, Washington, DC 20375

Zn-ferrite films, $\text{Zn}_x\text{Fe}_{3-x}\text{O}_4$ where the Zn:Fe ratio ranges from 0.36 to 0.76, were grown on glass substrates using a spin spray technique. Films are shown using scanning electron microscopy and atomic force microscopy to be dense and granular with an average grain size $\sim 0.3 \mu\text{m}$. X-ray diffraction indicates that the films are a $Fd3m$ symmetry consistent with a pure spinel ferrite phase. The films' coercive fields have a strong positive correlation with the film roughness indicating the dominance of a physical domain wall pinning mechanism. The films are smooth and magnetically soft near the ZnFe_2O_4 stoichiometry. All films, including those near the ZnFe_2O_4 stoichiometry, display ferrimagnetic behavior with compensation temperatures well above the bulk Neel temperature of 9.5 K; this is attributed to the cation disorder measured in the Zn cation distribution.

© 2002 American Institute of Physics. [DOI: 10.1063/1.1456428]

INTRODUCTION

Recent trends in microwave monolithic integrated circuit (MMIC) technology has focused on the integration of non-reciprocal devices (e.g., isolators and circulators) with active elements based on GaAs substrates. Since ferrites are typically processed at temperatures in excess of 900 °C, this demand has provided a significant challenge to microwave device engineers and materials scientists to fabricate ferrite structures having appropriate thickness (e.g., 10's microns) and high crystal quality at temperatures that do not degrade the GaAs-based devices (<450 °C).

One technique that has been shown to produce ferrite films of high crystalline quality at temperatures <100 °C is spin-spray deposition.¹ This technique was developed by Abe *et al.*^{2,3} of the Tokyo Institute of Technology and involves the reduction of metal salts onto a spinning substrate. Control of the precursor solution pH allows for tailoring of cation valency, phase selection, and phase purity of the resulting films. A review of this technique and variants of ferrite plating technology are presented in Refs. 1, 4, and 5.

MMIC needs are more likely to be met by low-loss spinel ferrite films such as the NiZn-ferrite (NZFO) system. However, prior to the processing of NZFO, one must first master the processing of the binary ferrite systems (i.e., Zn and Ni ferrites). This includes establishing conditions in which ZFO can be processed with tight stoichiometric control, phase purity, high density, and desirable film morphol-

ogy. These are the goals in the present study of the Zn-ferrite system.

There have been several studies of spin spray ferrite plating and related techniques in the synthesis and characterization of ferrite materials, including those of the NiZn-ferrite system.⁶⁻⁹ Limitations that were exposed in these studies include difficulties in processing films of the desired stoichiometry and control of equilibrium cation distributions.

EXPERIMENT

Films of $\text{Zn}_x\text{Fe}_{3-x}\text{O}_4$, where $x=0.8$ to 1.1, were processed by spin spray deposition onto glass substrates. The glass substrates were washed and rinsed in distilled water and soaked in chromic acid to remove any residual organic material. The substrates were then soaked again in an FeCl_2 solution to provide a seed layer for the growth of the spinel ferrite. Finally, these substrates were mounted onto a table that rotates at 300 rpm during growth and is held at a temperature of 80 °C. The temperature of the substrates was verified using an infrared thermometer.

An oxidizing solution of NaNO_2 was prepared and buffered to a pH of 8.2 using $\text{NH}_4(\text{C}_2\text{H}_3\text{O}_2)$ (ammonium acetate). This pH favors the precipitation and crystallization of spinel ferrites at 80 °C. Metal chloride precursor solutions of ZnCl_2 and FeCl_2 were prepared just prior to spraying to reduce the amount of uncontrolled conversion of Fe^{2+} to Fe^{3+} . The two solutions were mixed and sprayed at 50 ml/min for a period of 10 min.

Changing the ratio of metal chlorides in the precursor solutions allowed the variation of the film stoichiometry.

^{a)}Author to whom correspondence should be addressed; electronic mail: harris@anvil.nrl.navy.mil

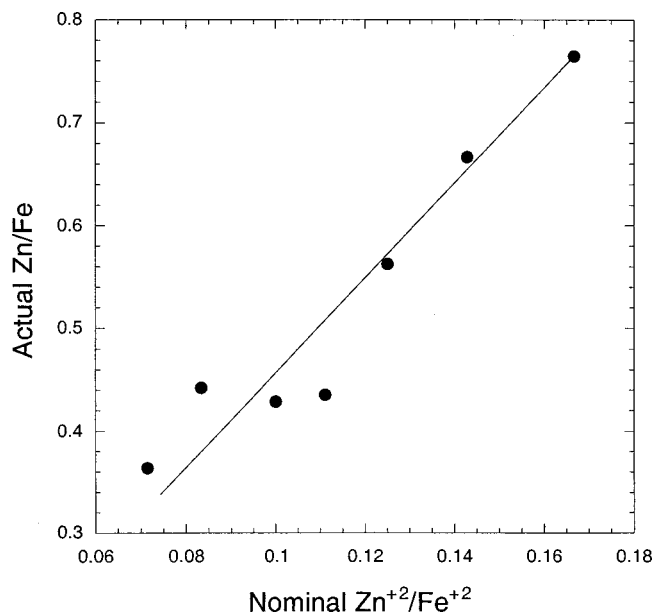


FIG. 1. Actual film stoichiometry as a function of the nominal Zn/Fe ratio defined by the ratio of the metal chloride precursor solutions.

The composition of the resulting films was determined by inductively coupled plasma (ICP) and x-ray fluorescence (XRF) spectroscopy within a SEM column. The film's long range structure was studied using θ - 2θ x-ray diffraction with using a $\text{Cu } K\alpha$ source, while the short range structure around the Zn cations was studied using extended x-ray absorption fine structure (EXAFS) spectroscopy. The EXAFS studies were performed using beamline X23B at the National Synchrotron Light Source (at Brookhaven National Laboratory) and followed the procedural steps outlined in Ref. 9.

Film morphology was examined using both contact mode atomic force microscopy and scanning electron microscopy.

The films' magnetic properties were studied using vibrating sample magnetometry to acquire room temperature hysteresis loops, while magnetic susceptibility was measured using a Quantum Design MPMS-5 SQUID magnetometer over a temperature range of 10 to 300 K with an applied field of 500 Oe. Hysteresis loops were collected at 10 K using the SQUID magnetometer.

RESULTS AND DISCUSSION

ICP and XRF measurements of the resulting films show that significant differences exist between the actual compositions and the ratio of precursor chloride solutions. Figure 1 is a plot of the nominal precursor solution ratio of Zn:Fe and the actual Zn:Fe ratio measured in the spinel ferrite films. As can be seen in Fig. 1, the uptake of Zn cations in the film is much greater than that of Fe cations. Hence, the relative amount of FeCl_2 is nearly five times greater than the ZnCl_2 solution to get the desired film composition.

The film morphology was found to vary from smooth and featureless to highly granular with acicular grains. For films having near the $\text{Zn/Fe}=0.5$ concentration, the films appear dense and granular with spherical grains ranging in

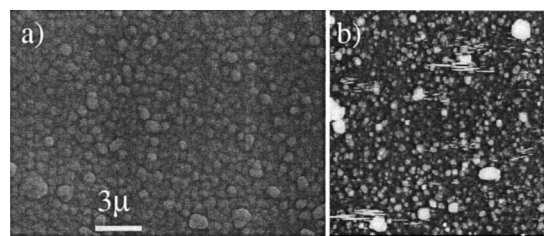


FIG. 2. (a) Scanning electron microscope image of the $\text{Zn}_{0.98}\text{Fe}_{2.02}\text{O}_4$ film sample displaying a dense, granular morphology. The image was collected using 10 keV electrons. The scale bar represents 3 μm . (b) Atomic force microscope image of the same sample. Data were collected in contact mode. The brightest areas of panel (b) represent a maximum vertical displacement of 300 nm.

size from from $\sim 0.2 \mu\text{m}$ to $\sim 2 \mu\text{m}$; the larger grains being relatively few in number. Figure 2 is an SEM micrograph of a sample having the ZnFe_2O_4 composition. The image in panel Fig. 2(a) was collected using, 10 keV electrons and a magnification of $\sim 5000 \times$. Figure 2(b) of the same figure contains an atomic force microscopy image of the same sample collected in contact mode. In this figure, the white intensity corresponds with a maximum height of 300 nm.

The long-range structure of the films was determined via x-ray diffraction (XRD) to be a close match to the spinel ferrite phase. In Fig. 3, the XRD profile of the $\text{Zn}_{0.98}\text{Fe}_{2.02}\text{O}_4$ sample in Fig. 2 is presented with all diffraction peaks of intensity greater than 1% (of maximum) indexed to the spinel phase ($Fd\bar{3}m$). No peaks appear that cannot be indexed to this phase.

Correspondingly, the short-range structure around the Zn cation is depicted in Fig. 4 as the Fourier transform of the Zn EXAES data. In this figure, the data corresponding to films having compositions $\text{Zn}_{0.98}\text{Fe}_{2.02}\text{O}_4$ are plotted with similar data collected from a NZFO made by the same technique.⁸⁻⁹ This comparison shows that the short-range symmetry of the Zn cations is indeed that of the spinel phase. However, the peaks appearing near 2.6 \AA (uncorrected for electron phase shifts) represents a population of Zn cations on the octahedral sublattice.⁹ Far fewer octahedral coordinated Zn cations appear in the NZFO film whereas in stoichiometric bulk

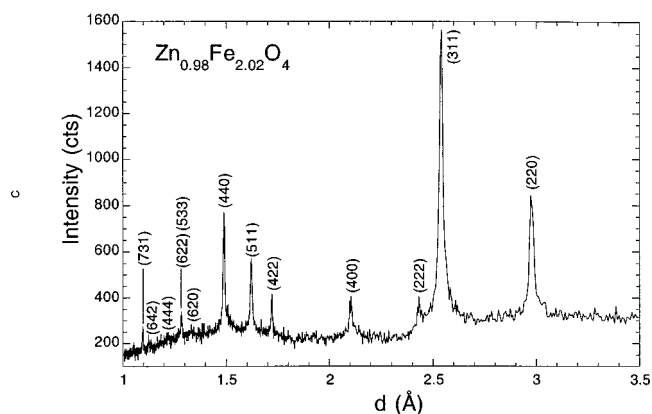


FIG. 3. θ - 2θ x-ray diffraction profile of a $\text{Zn}_{0.98}\text{Fe}_{2.02}\text{O}_4$ film collected using $\text{Cu } K\alpha$ radiation ($\lambda = 1.5406 \text{ \AA}$). The data are presented in d space ($d = \lambda/2 \sin \theta$). All diffraction features are indexed to the $Fd\bar{3}m$ space group of the spinel structure.

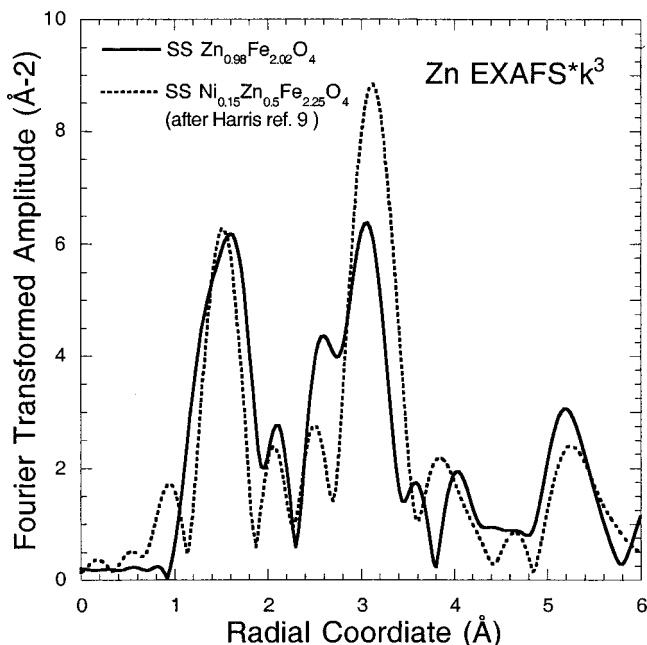


FIG. 4. Fourier transformed Zn EXAFS data collected from the $Zn_{0.98}Fe_{2.02}O_4$ film and a NiZn-ferrite film of Ref. 9. Both profiles are consistent with the local structure of the $Fd3m$ space group of spinel ferrites. Data have not been corrected for electron phase shifts.

ZFO, Zn cations reside solely on the tetrahedral sublattice. This indicates that a nonequilibrium cation distribution results from the spin-spray processing approach. An additional step of annealing these films after growth may be required to reduce the cation disorder.

In Fig. 5 the coercivity and the root mean squared roughness (R_{RMS}) of films are plotted against the actual film composition. In this plot one sees that as the Zn:Fe ratio approaches the stoichiometric concentration from either side (Zn rich or Zn depleted) the coercivity is reduced and the roughness decreases. One also sees that the coercivity and roughness are strongly positively correlated.

The strong correlation between the coercivity and the roughness suggest that the changes in coercivity arise from the physical pinning of magnetic domain walls likely due to grain boundaries. However, the role of cation disorder cannot be ruled out as a contributing mechanism.

The grain refinement that occurs for stoichiometries away from the ideal is unclear. However, one can envision that cation disorder incorporated during growth would create strain fields that limit grain size and cause local anisotropy fields, both of which would increase the coercivity.

SQUID magnetometry measurements indicate that all films show signs of ferrimagnetism with compensation temperatures well above the 9.5 K of the bulk Zn ferrite.¹⁰ As the

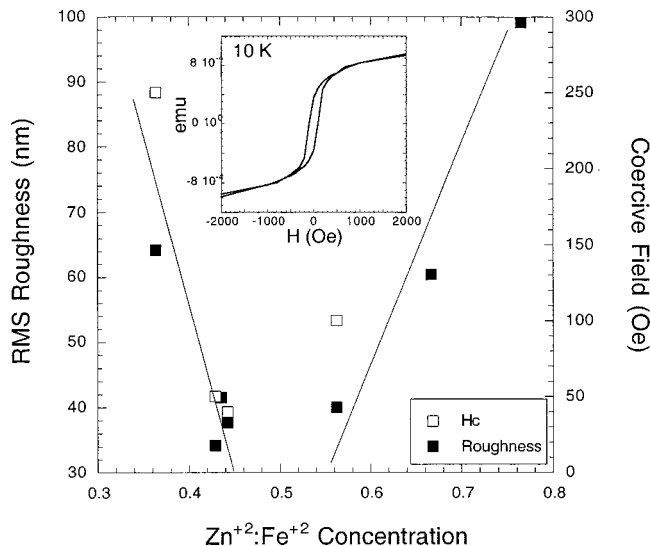


FIG. 5. Film root mean square roughness (R_{RMS}) and coercive field (H_c) of film samples plotted against the film composition. The inset plot is a hysteresis loop acquired at 10 K for the $Zn_{0.98}Fe_{2.02}O_4$ film showing the presence of hysteresis.

stoichiometry of the films approach 0.5 these temperatures decrease. The reason for magnetic activity well above the bulk Neel temperature is attributed to the cation disorder measured in Fig. 4. This creates a net moment on the tetrahedral sublattice strengthening the $A-B$ interaction and weakening the antiferromagnetic $B-B$ coupling (A =tetrahedral sublattice; B =octahedral sublattice). The enhancement of the Neel temperature by cation disorder in ZFO was also reported in ball-milled ZFO.¹¹

ACKNOWLEDGMENTS

This research was supported by the ONR and DARPA and was performed in part at the NSLS operated by the Department of Energy.

¹M. Abe, *Electrochim. Acta* **45**, 3337 (2000).
²M. Abe et al., *J. Appl. Phys.* **61**, 3211 (1987).
³M. Abe et al., *IEEE Trans. Magn.* **23**, 3736 (1987).
⁴M. Abe, T. Itoh, and Y. Tamaura, *Thin Solid Films* **216**, 155 (1992).
⁵M. Abe, *Suppl. J. Phys. (Colloque C2)* **7**, 467 (1997).
⁶C. M. Williams et al., *IEEE Trans. Magn.* **30**, 4896 (1994).
⁷Q. Zhang et al., *J. Appl. Phys.* **73**, 6248 (1993).
⁸V. G. Harris, N. C. Koon, C. M. Williams, Q. Zhang, M. Abe, and J. Kirkland, *Appl. Phys. Lett.* **68**, 2082 (1996).
⁹V. G. Harris, N. C. Koon, C. M. Williams, Q. Zhang, M. Abe, J. P. Kirkland, and D. A. McKeown, *IEEE Trans. Magn.* **31**, 3473 (1995).
¹⁰S. A. Oliver, V. G. Harris, H. Hamdeh, and J. C. Ho, *Appl. Phys. Lett.* **76**, 2761 (2000).
¹¹J. Smit and H. P. J. Wijn, *Ferrites* (Wiley, New York, 1959), and references contained within.